NASA TECHNICAL MEMORANDUM

NASA TM X-52665

NASA TM X-52665

N10K-00

AUGMENTATION OF SINGLE-PHASE HEAT TRANSFER IN TUBES BY USE OF HELICAL VANE INSERTS

by Martin U. Gutstein
Lewis Research Center
Cleveland, Ohio

and

George L. Converse and Jerry R. Peterson
Nuclear Systems Programs, General Electric Co.
Cincinnati, Ohio

TECHNICAL PAPER proposed for presentation at
Fourth International Heat Transfer Conference
Versailles/Paris, France, August 31-September 5, 1970

AUGMENTATION OF SINGLE-PHASE HEAT TRANSFER IN TUBES BY USE OF HELICAL VANE INSERTS

by Martin U. Gutstein
Lewis Research Center
Cleveland, Ohio

and

George L. Converse and Jerry R. Peterson
Nuclear Systems Programs, General Electric Co.
Cincinnati, Ohio

TECHNICAL PAPER proposed for presentation at

Fourth International Heat Transfer Conference
Versailles/Paris, France, August 31-September 5, 1970

NATIONAL AERONAUTICS AND SPACE ADMINISTRATION

AUGMENTATION OF SINGLE-PHASE HEAT TRANSFER IN TUBES BY USE OF HELICAL VANE INSERTS

Martin J. Gutstein
NASA Lewis Research Center, Cleveland, Ohio
and
George L. Converse and Jerry R. Peterson
Nuclear Systems Programs, General Electric Co., Cincinnati, Ohio

Abstract

The pressure drops and heat transfer coefficients of helical vane inserts of four different pitch-tube diameter ratios were measured over a Reynolds number range of about 30,000 to 300,000. The heat transfer coefficients and the pressure drops increased with increasing mass flow rate and decreasing insert pitch-tube diameter ratio. A momentum analysis, based on solid body rotation, resulted in new expressions for the momentum and frictional pressure drops for fully-developed flow in these inserts. Helical vane friction factors and Stanton numbers, computed from the experimental data in accordance with parameters derived from the analysis, correlated with conventional plain tube expressions.

INTRODUCTION

High-temperature, liquid-metal boilers for space electric powerplants are required to be as compact and light weight as possible. To achieve these goals, swirl-generating inserts are used inside the tubes of these boilers. The inserts enhance the heat transfer processes in the boiling fluid, particularly in the all-vapor (superheat) region of the boiler (refs. 1 and 2). Substantial savings of boiler size and weight are made possible through the use of these inserts. Examples of the types of swirl inserts which have been or are contemplated for use in space boilers are the twisted tape, the wire coil, and the helical vane. These are illustrated in figure 1. The inserts shown in the figure may be classified as "passive" devices. That is, the heat transfer enhancement observed with the use of swirl inserts is due to the rotational velocity imparted to the fluid; the fin conduction effect being generally small.

The helical vane insert, consisting of a single vane wrapped about a supporting rod or centerbody, possesses several advantages over the other two insert configurations. This insert creates a single (mathematically), well-defined helical flow passage in contradistinction to the twisted tape or wire coil. Fluid maldistribution between the two flow passages formed in a tube by the twisted tape, as has been observed by the authors, cannot occur with the helical vane. Substantial bypassing, which is indicated by the heat transfer data for the wire coil (ref. 3), likewise is not possible for this insert; all of the flow must follow the helical passage formed by the insert. Consequently, more reliable predictions and extrapolations of the thermal and hydraulic performance of the helical vane insert can be expected.

Because of the factors just cited and a complete absence of data in the literature, the authors undertook an experimental and analytical investigation of the single-phase heat transfer and pressure loss characteristics of the helical vane insert. A more comprehensive discussion of this investigation is presented in reference 4.

EXPERIMENTAL APPARATUS

The apparatus employed in the experiments is shown schematically in figure 2. Air, from the supply, flowed through a pressure regulator, a standard A.S.M.E. orifice, a control valve, and flow straightener before entering the test section. The orifice pressure differences were measured with a 60-inch (1.5 m) water manometer. Absolute pressures upstream of the orifice were measured with a calibrated Bourdon tube gage.

The test section consisted of a stainless steel tube 1.96 meters long with an outer diameter of 2.54 centimeters and a wall thickness of 1.65 millimeters. Two pressure taps were positioned 1.118±0.003 meters apart with the downstream tap 13 cm from the end of the tube. The inside of the tube was carefully polished in the vicinity of the pressure taps to insure the absence of burrs. A 30-inch (76-cm) water manometer and a 100-inch (2.54-m) mercury manometer were employed to measure test section pressure loss. Test section exit absolute pressure was measured with a 30-inch (76-cm) mercury manometer.

The heated zone of the test section was 1.016±0.003 m long and located symmetrically within the pressure taps. Heat was applied over this length by Inconel-sheathed 20-gage Chromel heating wire. Approximately 15.25 m of the 0.25 cm o.d. heating wire were wrapped around the test section. The distance between adjacent wire turns was uniformly 0.64 cm except for six turns at each end where one-half of this spacing was employed. Assembly of the test section was completed by application of a 0.64-cm thickness of high-conductivity refractory cement and a 5.1-cm layer of thermal insulation. Electrical power inputs up to 4 kilowatts were employed with this arrangement, equivalent to heat flux levels up to 3940 W/m^2.

Four thermocouple stations were provided on the test section, one to determine inlet air temperature and three providing local wall temperature measurements in the heated zone. Each station was comprised of three bare wire Chromel-Alumel thermocouples positioned uniformly around the tube circumference. The inlet air thermocouple station was located 51 cm upstream of the start of the heated zone. The three heated-zone thermocouple stations were located approximately equidistant within the heated zone. All test section thermocouples were calibrated in place before start of testing. The heat transfer data presented in this report are based on the temperature measurements made at the inlet air temperature station and the station located at the mid-point of the test section.

Four helical vane inserts were tested in the same stainless steel tube described above. The pitch (axial distance traversed for a 2π revolution of the vane)-to-tube inner diameter ratios (Y/D_w) of the four inserts were: 0.52, 0.75, 1.46, and 6.36. The diameter of the centerbody of the four inserts was approximately 0.6 cm. The length of the inserts was typically 1.8 m, of which about 50 cm extended upstream of the first pressure tap and provided a flow development length.

DISCUSSION OF RESULTS

Pressure Losses and Heat Transfer Coefficients in the Plain Tube

To validate the experimental techniques employed in this investigation, friction factors and Stanton numbers were computed from the plain tube data. These were then plotted as a function of Reynolds number and compared with

standard correlations. The friction factors for the plain tube were compared with Prandtl's universal law of friction for smooth pipes (ref. 5), given below

$$\frac{1}{\sqrt{f_o}} = 2.0 \log_{10}\left(Re_o\sqrt{f_o}\right) - 0.8 \tag{1}$$

The Stanton numbers computed from the data were compared with the following correlation:

$$j_o = (St_o)(Pr)^{0.6} = 0.023(Re_o)^{-0.2} \tag{2}$$

The experimental friction factors and Stanton numbers fell within about 10 percent of the values predicted by the correlations over the range of Reynolds numbers from 30,000 to 300,000. This agreement and the relatively small data scatter showed the measurements and data reduction procedures to be adequately accurate and precise.

Frictional Pressure Losses in Helical Vane Inserts

The overall pressure loss across the test section consisted of a frictional pressure drop and a momentum loss. To compute the friction factors for the plain tube, the momentum pressure loss had to be subtracted from the overall pressure drop. Likewise, to calculate the friction factors for the inserts which were tested, an appropriate helical flow momentum pressure drop had to be estimated. This pressure loss was obtained from a momentum conservation analysis which is briefly described below and is derived in reference 4.

The analysis assumed that the fluid rotates around the tube axis at a constant angular speed (solid-body rotation) and translates at a constant average velocity. In addition, helical streamlines within the fluid were assumed parallel to the insert vane. The analysis was therefore predicated on fully developed steady flow. By virtue of these assumptions, the fluid helical velocity, V_H, was resolved into an axial component, $V_{z,H}$, and a tangential velocity, V_θ. The axial velocity was obtained from continuity. The tangential and helical velocities were related to the axial velocity by the geometry of the insert and both were functions of the radial displacement from the tube centerline. The equations relating $V_{z,H}$, V_θ, and V_H are shown below.

$$V_{z,H} = \left(\frac{m}{A_{c,H}\rho}\right) \tag{3}$$

$$V_\theta = \left(\frac{2\pi r}{Y} V_{z,H}\right) = \left[\left(\frac{\ell_\theta}{\ell_z}\right) V_{z,H}\right] \tag{4}$$

$$V_H = \left\{\frac{\left[Y^2 + (2\pi r)^2\right]^{1/2}}{Y} V_{z,H}\right\} = \left[\left(\frac{\ell_H}{\ell_z}\right) V_{z,H}\right] \tag{5}$$

$$V_H = \left(V_{z,H}^2 + V_\theta^2\right)^{1/2} \tag{6}$$

The maximum helical velocity occurs at the tube inner radius, r_w, as shown in equation (7).

$$V_{H,w} = \left\{ \frac{\left[Y^2 + (2\pi r_w)^2\right]^{1/2}}{Y} V_{z,H} \right\} = \left[\left(\frac{\ell_{H,w}}{\ell_z} \right) V_{z,H} \right] \tag{7}$$

Utilizing the above expressions for the velocity distribution within a helical insert, conservation of linear and angular momentums was applied to a control volume of the fluid. The two conservation equations resulted in an expression for the pressure loss across an axial increment of the helical insert. This equation consisted of separable momentum and frictional pressure loss terms. The momentum pressure loss term as derived from the analysis was

$$\Delta P_{m,H} = \frac{m^2}{A_{c,H}^2 g_c} \left(\frac{1}{\rho_e} - \frac{1}{\rho_i} \right) \left[1 + \frac{2\pi^3}{Y^2} \frac{\left(r_w^4 - r_{cb}^4 \right)}{A_{c,H}} \right] \tag{8}$$

Equation (8) was employed to calculate the momentum pressure losses which occurred in the insert test sections. These losses were then subtracted from the measured overall static pressure losses to obtain the frictional pressure drops, $\Delta P_{f,H}$.

Friction factors and corresponding Reynolds numbers for the four helical vane inserts which were tested were computed by two methods. The first was based on the following set of equations.

$$f_A = \frac{\Delta P_{f,H}}{\bar{\rho} \left(\frac{V_{z,A}^2}{2 g_c} \right) \frac{\ell_z}{D_w}} \tag{9}$$

$$Re_A = \frac{D_w V_{z,A} \bar{\rho}}{\bar{\mu}} \tag{10}$$

$$V_{z,A} = \frac{m}{A_{c,A} \bar{\rho}} \tag{11}$$

The flow cross sectional area, $A_{c,A}$, is defined by

$$A_{c,A} = \frac{\pi}{4} \left(D_w^2 - D_{cb}^2 \right) - \frac{t}{2} \left(D_w - D_{cb} \right) \tag{12}$$

The first method attributes the frictional pressure losses to the axial component of the fluid velocity and to the axial length traversed by the flow.

Figure 3 presents the plot of friction factors versus Reynolds numbers for the helical vane inserts reduced in accordance with equations (9) to (12). Equation (1), the correlation of friction factors for smooth tubes, is likewise plotted for reference. The friction factors computed by this first method are clearly greater than the smooth tube line although their trend with Reynolds number appears similar. The displacement of the data from the correlation increases with decreasing pitch-to-tube diameter ratio.

The second method used to calculate friction factors and Reynolds numbers was based on the momentum analysis. From that analysis, the friction factor for a finite axial length increment was

$$f_H = \frac{\Delta P_{f,H}}{\bar{\rho}\frac{V_{z,H}^2}{2g_c}\left(\frac{\ell_{H,w}}{\ell_z}\right)^3\frac{\ell_z}{D_H}} \tag{13}$$

The hydraulic diameter for a helical vane insert was defined as

$$D_H = \frac{4A_{c,H}}{\left[p_w + \left(\frac{\ell_{H,cb}}{\ell_{H,w}}\right)^3 p_{cb} + 2\left(\frac{\ell_z}{\ell_{H,w}}\right)^3 \int_{r_{cb}}^{r_w}\left(\frac{\ell_H}{\ell_z}\right)^4 dr\right]} \tag{14}$$

where the terms p_w and p_{cb} are the wetted perimeters of the tube wall and insert centerbody, respectively.

The flow cross sectional area, $A_{c,H}$, required for calculation of the axial velocity and equivalent diameter is

$$A_{c,H} = \pi\left(r_w^2 - r_{cb}^2\right) - \int_{r_{cb}}^{r_w} t(\ell_H/\ell_z)dr \tag{15}$$

Equation (13) defining the helical vane friction factor may be written in a different form by substitution of equation (7)

$$f_H = \frac{\Delta P_{f,H}}{\bar{\rho}\frac{V_{H,w}^2}{2g_c}\frac{\ell_{H,w}}{D_H}} \tag{16}$$

As equation (16) indicates, the second method evaluates the friction factor employing both the maximum helical velocity, $V_{H,w}$, which occurs near the tube wall and the maximum helical path length, $\ell_{H,w}$. Moreover, the equivalent hydraulic diameter differs from the conventional expression in that the wetted perimeters of the tube wall, vane and centerbody surfaces are weighted in accordance with the fluid helical velocities adjacent to these surfaces. Because of the similarity of equations (9) and (16), the Reynolds number for flow in a helical vane insert was defined as

$$Re_H = \frac{D_H V_{H,w}\bar{\rho}}{\bar{\mu}} = \frac{D_H V_{z,H}(\ell_{H,w}/\ell_z)\bar{\rho}}{\bar{\mu}} \tag{17}$$

Helical friction factors and Reynolds numbers were computed from the frictional pressure drop data of the four inserts. These are shown plotted in figure 4 along with the line corresponding to friction factors for smooth tubes. It is evident from this figure that the second method, based on the helical flow parameters discussed above, suitably correlates the experimental data with the Prandtl's equation. The deviation of the friction factors from the smooth-tube correlation is about ±10 percent in the Reynolds number range of 30,000 to 300,000. Thus, equation (1) may be rewritten for helical vane inserts as

$$\frac{1}{\sqrt{f_H}} = 2.0\log_{10}\left(Re_H\sqrt{f_H}\right) - 0.8 \tag{18}$$

Heat Transfer Coefficients of Helical Vane Inserts

The correlation of the insert heat transfer coefficients with helical flow parameters was achieved by modifying equation (2), as shown below, and employing equation (17) for the Reynolds number.

$$j_H = (St_H)(Pr)^{0.6} = \left[\frac{h}{c_p \bar{\rho} V_{z,H}(\ell_{H,w}/\ell_z)}\right]\left(\frac{c_p \bar{\mu}}{k}\right)^{0.6} \tag{19}$$

Application of equations (19) and (17) to the data was justified by the Reynolds analogy (ref. 5) and the success in correlating the measured friction factors with helical parameters.

Figure 5 presents the heat transfer data for the four insert configurations reduced in accordance with equations (19) and (17). Again, the conventional relationship for smooth tubes (eq. (2)), is plotted along with the experimental data. Figure 5 illustrates that a modified equation, such as equation (20) below, can reasonably predict the heat transfer coefficients in helical vane inserts.

$$\left[\frac{h}{c_p \rho V_{z,H}(\ell_{H,w}/\ell_z)}\right]\left(\frac{c_p \mu}{k}\right)^{0.6} = 0.023\left[\frac{D_H V_{z,H}(\ell_{H,w}/\ell_z)\rho}{\mu}\right]^{-0.2} \tag{20}$$

The deviations of the data from the correlation in figure 5 are generally less than 20 percent in the Reynolds number range of 30,000 to 300,000. Application of equation (20) is limited to passive helical inserts of the type reported herein. For helical inserts in which the vane makes good thermal contact with the tube wall, an appropriate expression accounting for the conduction effect must be formulated.

Normalized Helical Insert Frictional Pressure Drops and Heat Transfer Coefficients

The frictional pressure drops and heat transfer coefficients for the insert geometries of this study, given by equations (13), (18), and (20), were normalized on the basis of equal axial length, mass flow rate and fluid properties to corresponding expressions for plain tube frictional pressure drop and heat transfer. These normalizations are shown in figures 6 and 7, respectively. In addition, figures 6 and 7 each contain four data points corresponding to the values of $\Delta P_{f,H}/\Delta P_{f,o}$ and h/h_o obtained from the experiments. In general, the agreement of the experiments and theory is satisfactory. The deviation of the experimental data appears to increase with increasing pitch-tube diameter ratio. This may be due to secondary flows induced by the helical vane inserts and not accounted for in the analysis.

CONCLUDING REMARKS

A series of careful experiments has been conducted to measure the overall pressure losses and local heat transfer coefficients of air flowing inside a tube containing helical vane inserts. Four helical vane inserts were tested having pitch-tube inner diameter ratios of 0.52, 0.75, 1.46, and 6.36. The tests were conducted over a range of Reynolds numbers of 30×10^3 to 300×10^3. The experimental data indicate that both the pressure losses and

the heat transfer coefficients increased substantially as the insert pitch-to-tube diameter ratio decreased.

An analysis was performed employing conservation of momentum in the axial and angular directions. Solid-body rotation and constant translational velocity were assumed. This analysis yielded new expressions for fully-developed, helical vane insert momentum and frictional pressure losses. The analysis showed that the major contribution to the frictional pressure loss in swirl-generating inserts arises from the shear stresses near the tube wall surface where the fluid helical velocities are the largest. Lesser contributions are made by the shear stresses along the vane and insert centerbody. The analysis did not account for secondary flows induced by the helical vane insert.

Helical vane friction factors, computed from the experimental data in accordance with the parameters determined from the analysis, correlated with a conventional expression for friction factors in smooth, plain tubes. In the range of Reynolds numbers from 30,000 to 300,000, the deviation of the experimental friction factors from the correlating expression was about ±10 percent. A comparable correlation of helical vane insert Stanton numbers, computed from the data, with a conventional expression for plain tube coefficients was likewise achieved. In general, the experimental Stanton numbers deviated less than 20 percent from the correlating line.

NOMENCLATURE

$A_{c,A}$	approximate flow cross sectional area with helical vane insert taken perpendicular to tube axis	k	thermal conductivity
		ℓ	length
		m	mass flow rate
$A_{c,H}$	true flow cross sectional area with helical vane insert taken perpendicular to tube axis	P	pressure
		Pr	Prandtl number
c_p	specific heat capacity	p	perimeter
D	diameter	Re	Reynolds number
D_H	equivalent hydraulic diameter of helical vane insert	r	tube radius
		St	Stanton number
f	friction factor	t	vane thickness
g_c	conversion factor	V	fluid velocity
h	heat transfer coefficient of helical vane insert	Y	insert pitch-axial length for 360° revolution of vane
h_o	heat transfer coefficient of plain tube		
j	Stanton-Prandtl modulus, $(St)(Pr)^{0.6}$		

Greek Notation

θ	tangential or angular
ρ	density
$\bar{\rho}$	average density
μ	viscosity
$\bar{\mu}$	average viscosity

Subscripts

cb	centerbody
e	exit
f	frictional
H	helical or helical vane
i	inlet
m	momentum
o	plain tube
w	tube inner surface
z	axial

ACKNOWLEDGEMENT

This paper is based on work conducted under National Aeronautics and Space Administration-Lewis Research Center Contract NAS 3-9426.

REFERENCES

[1] J. R. Peterson: High-Performance "Once-Through" Boiling of Potassium in Single Tubes at Saturation Temperatures of 1500° to 1750° F. NASA Cr-842 (1967).

[2] J. A. Bond, and G. L. Converse: Vaporization of High-Temperature Potassium in Forced Convection at Saturation Temperatures of 1800° to 2100° F. NASA CR-843 (1967).

[3] E. Sams: Heat Transfer and Pressure-Drop Characteristics of Wire-Coil Type Turbulence Promoters. Presented at USAEC Reactor Heat Transfer Conference, New York, N.Y. (Nov. 1956).

[4] M. Gutstein, G. Converse, and J. Peterson: The Pressure Drop and Heat Transfer Performance of Helical Vane Inserts. NASA TN (To be published).

[5] H. Schlichting: Boundary Layer Theory. McGraw-Hill, 4th ed. (1960).

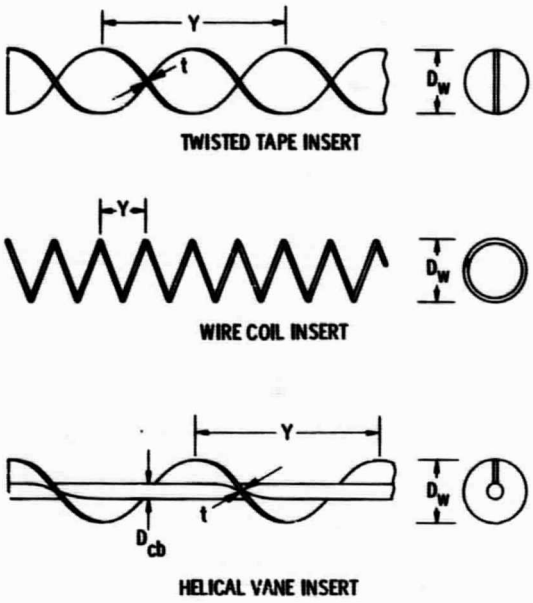

Figure 1. - Sketch of twisted tape, wire coil and helical vane inserts.

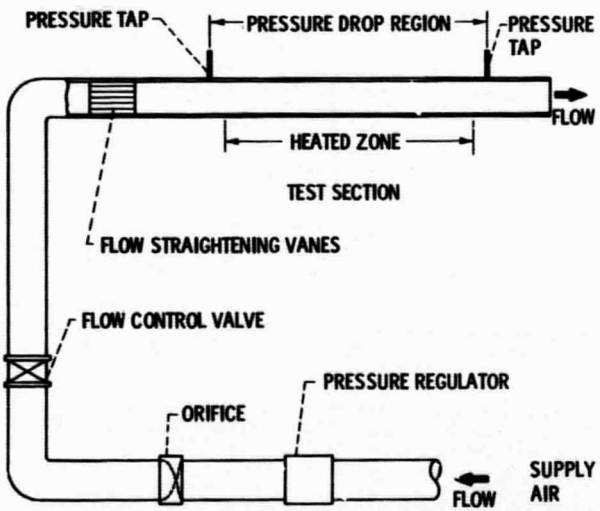

Figure 2. - Schematic diagram of test apparatus.

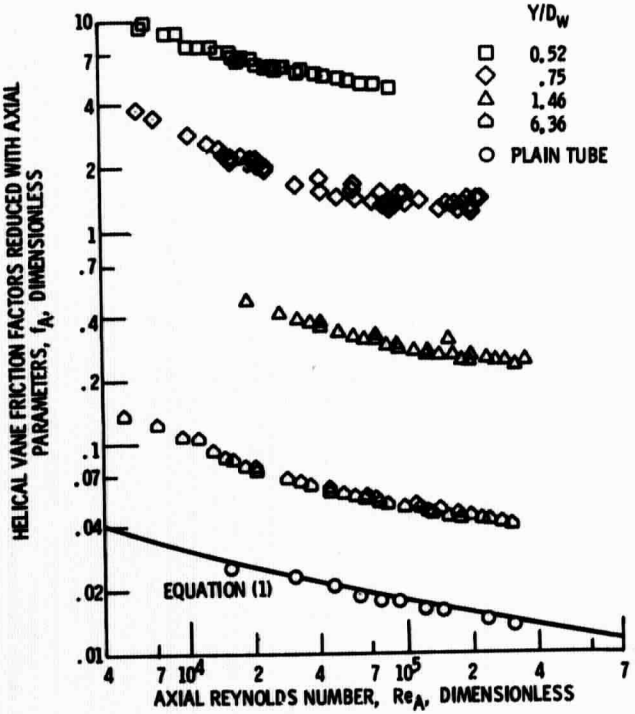

Figure 3. - Helical vane friction factors reduced with axial parameters.

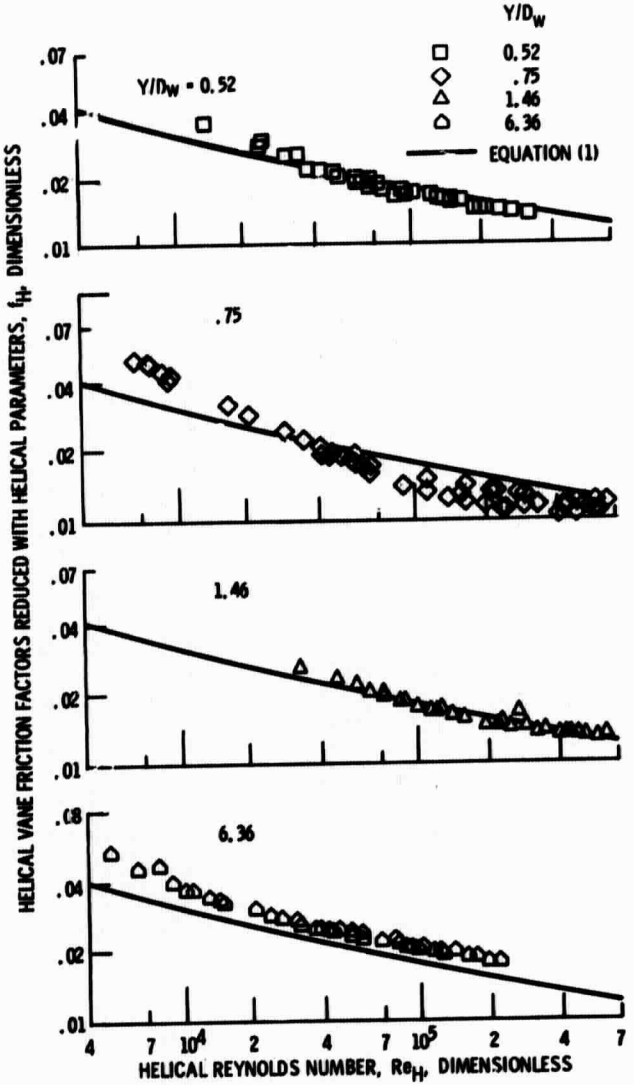

Figure 4. - Helical vane friction factors reduced with helical parameters.

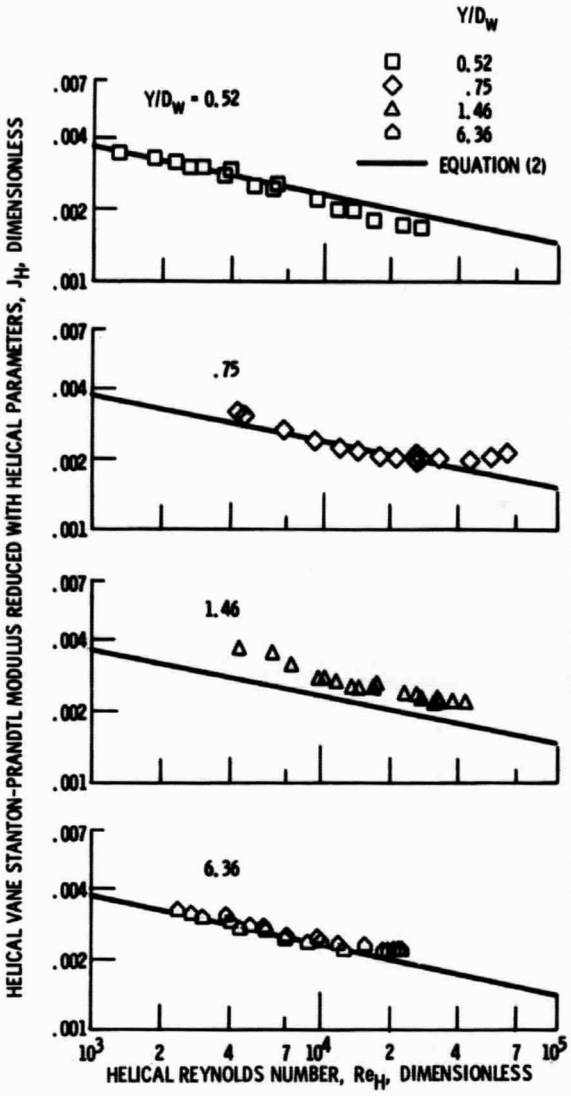

Figure 5. - Helical vane Stanton-Prandtl modulus as a function of Reynolds number reduced with helical parameters.

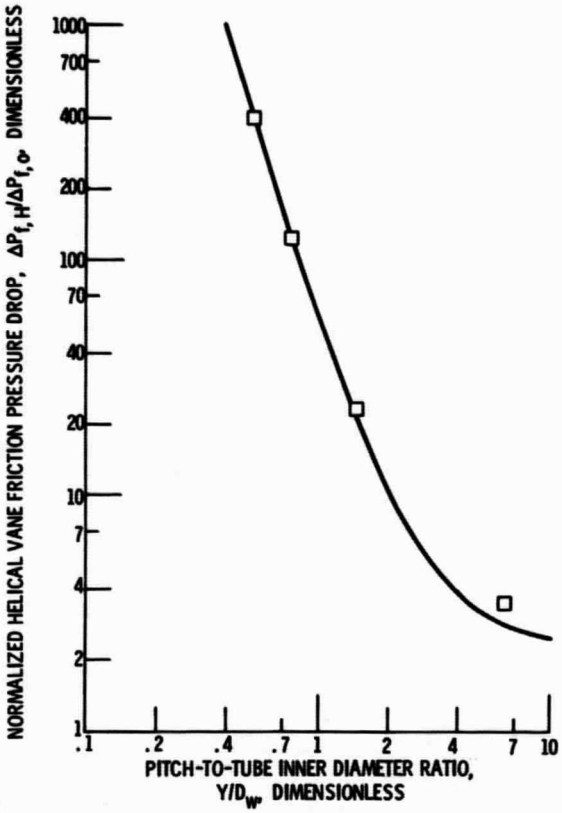

Figure 6. - Frictional pressure drops for the helical vane inserts normalized to plain tube frictional pressure drops.

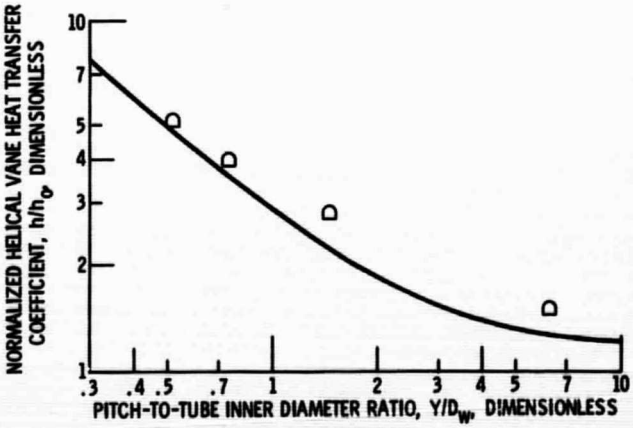

Figure 7. - Heat transfer coefficients for the helical vane inserts normalized to the plain tube coefficients.

NASA-CLEVELAND, OHIO E-5253